

See discussions, stats, and author profiles for this publication at: <https://www.researchgate.net/publication/263944381>

A Screened Hybrid DFT Study of Actinide Oxides, Nitrides, and Carbides

ARTICLE in THE JOURNAL OF PHYSICAL CHEMISTRY C · JUNE 2013

Impact Factor: 4.77 · DOI: 10.1021/jp403141t

CITATIONS

6

READS

77

5 AUTHORS, INCLUDING:



Xiao-Dong Wen

Institute of Coal Chemistry, Chinese Academy of Sciences

98 PUBLICATIONS 933 CITATIONS

SEE PROFILE



Richard L Martin

Los Alamos National Laboratory

441 PUBLICATIONS 25,733 CITATIONS

SEE PROFILE



Sven P. Rudin

Los Alamos National Laboratory

65 PUBLICATIONS 501 CITATIONS

SEE PROFILE



Enrique R Batista

Los Alamos National Laboratory

99 PUBLICATIONS 2,171 CITATIONS

SEE PROFILE

A Screened Hybrid DFT Study of Actinide Oxides, Nitrides, and Carbides

Xiao-Dong Wen,[†] Richard L. Martin,^{*,†} Gustavo E. Scuseria,^{‡,§} Sven P. Rudin,[†] and Enrique R. Batista[†]

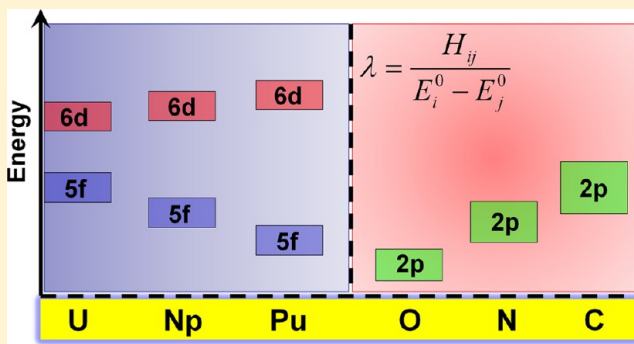
[†]Theoretical Division, Los Alamos National Laboratory, Los Alamos, New Mexico 87545, United States

[‡]Department of Chemistry, Department of Physics and Astronomy, Rice University, Houston, Texas 77251-1892, United States

[§]Chemistry Department, Faculty of Science, King Abdulaziz University, Jeddah 21589, Saudi Arabia

S Supporting Information

ABSTRACT: A systematic study of the structural, electronic, and magnetic properties of actinide oxides, nitrides, and carbides (AnX_{1-2} with $\text{X} = \text{C}, \text{N}, \text{O}$) is performed using the Heyd–Scuseria–Ernzerhof (HSE) hybrid functional. Our computed results show that the screened hybrid HSE functional gives a good description of the electronic and structural properties of actinide dioxides (strongly correlated insulators) when compared with available experimental data. However, there are still some problems reproducing the electronic properties of actinide nitrides and carbides (strongly correlated metals). In addition, in order to compare with the results by HSE, the structures, electronic, and magnetic properties of these actinide compounds are also investigated in the PBE and PBE+U approximation. Interestingly, the density of states of UN obtained with PBE compares well with the experimental photoemission spectra, in contrast to the hybrid approximation. This is presumably related to the need of additional screening in the Hartree–Fock exchange term of the metallic phases.



1. INTRODUCTION

The actinide (U, Np, Pu) oxides, nitrides, and carbides are of both fundamental and applied interest. These actinide materials are members of a class of strongly correlated materials—while the early dioxides are Mott insulators, the later ones, beginning with Pu, are charge-transfer insulators. The mononitrides and carbides are generally metals; the nitrides (and perhaps the carbides) are strongly correlated. Technological interest in these materials stems from their use or potential use as advanced nuclear fuels. The actinide nitrides and carbides may be the ideal fuel candidates for certain generation IV reactors.¹ It is unfortunately true, however, that their physical and chemical complexity make them extremely challenging to characterize experimentally or theoretically. A number of basic properties associated with their electronic structure are still not known; this includes magnetic ordering and optical gaps.

The development of a first-principles predictive capability for strongly correlated materials (Mott insulators and correlated metals) is one of the grand challenges in electronic structure theory. Over the past decade significant progress has been made on the Mott insulator front. We have recently reviewed the predictions of DFT+U, self-interaction correction (SIC), dynamic mean field theory (DMFT), and the Heyd–Scuseria–Ernzerhof (HSE) screened hybrid density functional with respect to the properties of actinide dioxides^{2,3}

and U_3O_8 phases.⁴ We find that HSE, in particular, provides a more balanced and overall quite satisfactory description of geometries, densities-of-states, and optical band gaps for these insulators. In this paper, we turn our attention to the metallic actinide compounds, exemplified by the strongly correlated metal UN. Previously unpublished results for the actinide monoxides are also reported here. We utilize the HSE functional⁵ implemented in VASP (Vienna Ab-initio Simulation Package).⁶ The details of the PAW potentials and plane-wave basis sets are as described previously.^{2,4} The effect of spin–orbit coupling will be discussed in more detail in a subsequent publication, but we note that it had little effect on the properties reported here in the dioxide series.² The HSE parameters are universal, material independent, and reported in the original work.⁷

2. RESULTS AND DISCUSSIONS

2.1. Actinide Oxides, Rocksalt AnO ($\text{An} = \text{U}, \text{Np}$, and Pu). Table 1 summarizes the calculated relative energies for antiferromagnetic (AFM), ferromagnetic (FM), and non-magnetic (NM) states; lattice constants (\AA); magnetic moment (μ_B); and band gap (eV) of actinide monoxides using HSE.

Received: March 30, 2013

Revised: May 31, 2013

Table 1. Calculated Relative Energy (eV per AnO_2 or AnO , where $\text{An} = \text{U}$, Np , and Pu), Lattice Constants (\AA), Magnetic Moment (μ_B), and Band Gap (eV) Using HSE

		magn state	$E_{\text{rel.}}$ (eV per AnO_2)	a_0 (Å)	μ (μ_B)	E_{gap} (eV)
AnO_2	UO_2	AFM ^a	0.00	5.458	1.98	2.4
		FM	0.77	5.418		
		NM	1.72	5.326		
		expt		5.470 ⁸	1.8 ⁹	2.1 ¹⁰
	NpO_2	AFM ^a	0.00	5.412	3.00	2.6
		FM	−0.12	5.411		
		NM	1.41	5.400		
		expt		5.434 ¹¹	0.4 ¹²	2.85 ¹³
	PuO_2	AFM ^a	0.00	5.383	4.00	2.4
		FM	0.15	5.378		
		NM	2.79	5.350		
		expt		5.398 ¹⁴	0.00 ¹⁵	2.80 ¹³
		magn state	$E_{\text{rel.}}$ (eV per AnO)	a_0 (Å)	μ (μ_B)	E_{gap} (eV)
AnO	UO	AFM ^a	0.00	4.902	2.10	0.0
		FM	0.19	4.906		
		NM	1.19	4.782		
		expt		4.920 ¹⁶	—	—
	NpO	AFM ^a	0.00	4.867	3.50	0.0
		FM	0.00	4.867		
		NM	2.44	4.750		
		expt		5.010 ¹⁷		
	PuO	AFM ^a	0.00	4.927	4.00	0.0
		FM	0.16	5.004		
		NM	3.64	4.787		
		expt		4.960 ¹⁸	—	—

^aA small tetragonal disorder with $a = b \neq c$ is found in AFM states.

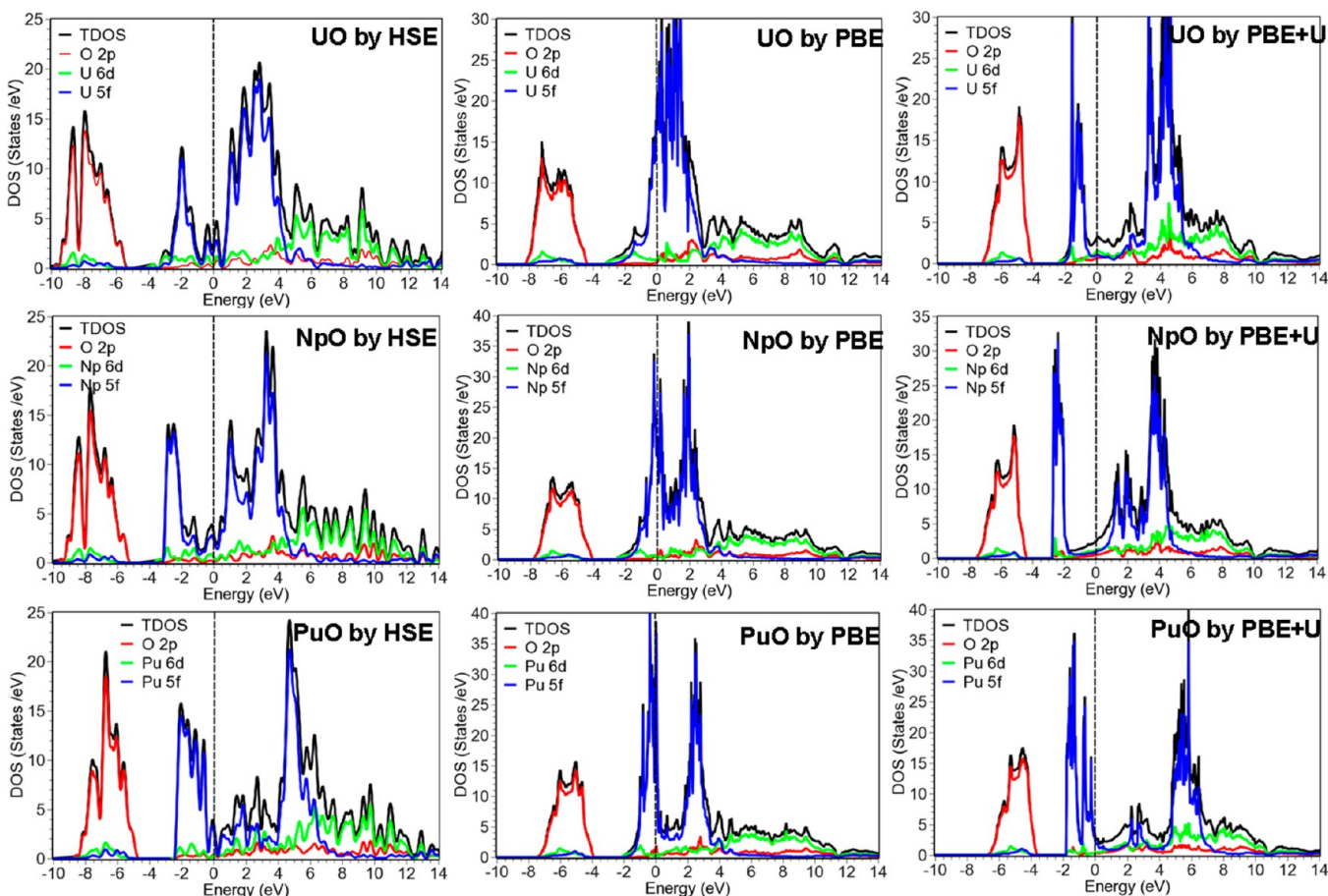


Figure 1. Calculated density of states of the corresponding most stable states AnO ($\text{An} = \text{U}$, Np , and Pu) obtained with HSE, PBE, and PBE+U ($U_{\text{eff}} = 4$ eV). Note that the highest occupied level is adjusted to zero.

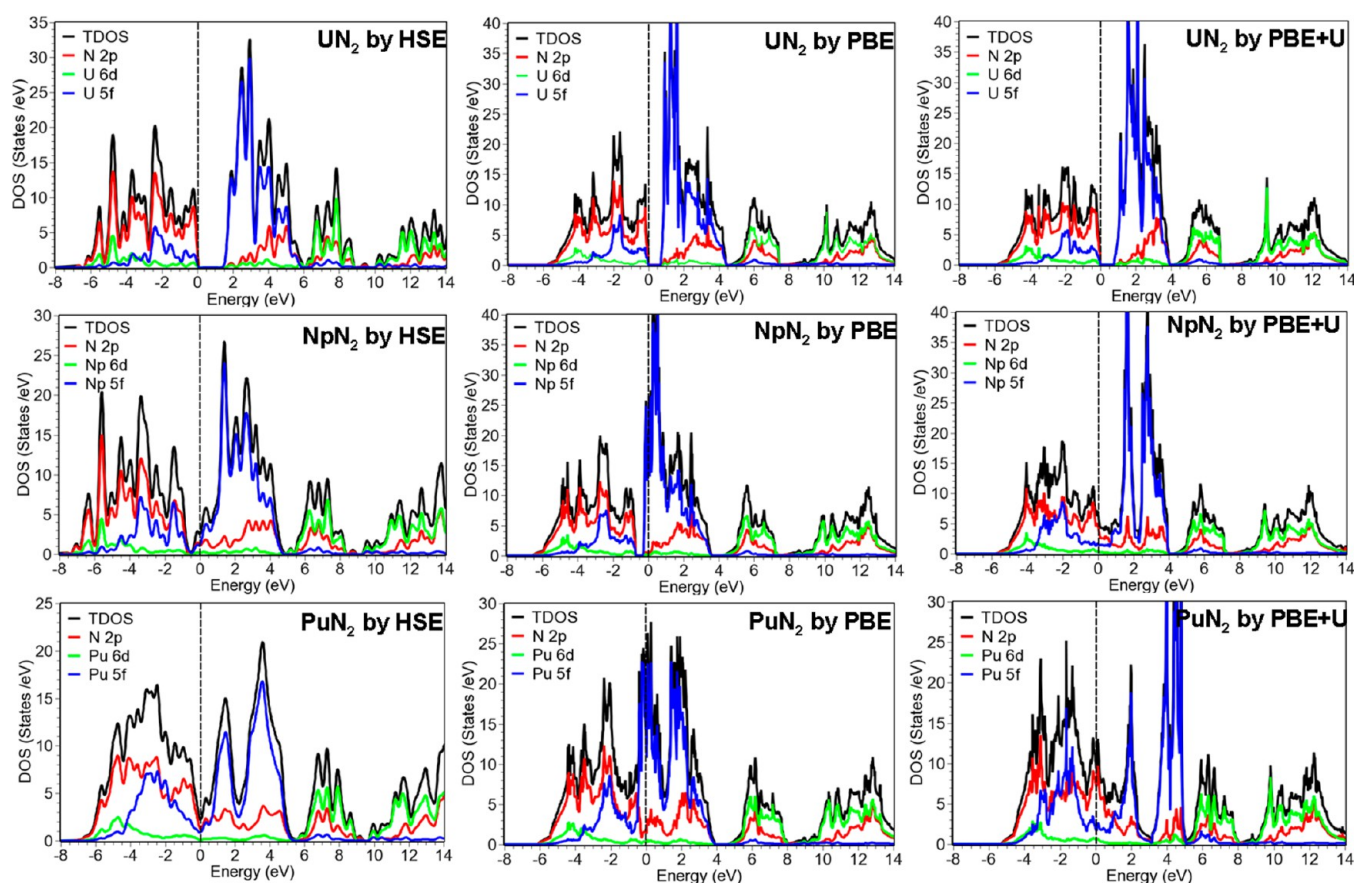


Figure 2. Calculated density of states of the corresponding most stable state of AnN_2 ($An = U, Np$, and Pu) obtained with HSE, PBE, and PBE+U ($U_{\text{eff}} = 4$ eV).

We also include for completeness our earlier results on the dioxides.² HSE finds the rocksalt AnO materials to be metallic, with AFM ordering along (100) (see the Supporting Information for details). The exception in the magnetic ordering occurs for NpO , where HSE finds no significant preference for the AFM over the FM state. Interestingly, the lattice constants of the three actinide monoxides obtained with HSE are underestimated when compared with experimental data, as shown in Table 1. The density of states computed with HSE (see Figure 1) for the three monoxides show a small density of An 5f states at the Fermi level, which is similar to the results obtained with PBE+U. However, this is in contrast to the results for the PBE generalized-gradient approximation, where sharp 5f peaks are seen at the Fermi energy in all three actinide monoxides. As is the case in the dioxides,² all three approximations separate the O 2p and U 5f quite distinctly in the uranium case, with the O 2p and An 5f densities merging in the later members.

2.2. Actinide Nitrides, Fluorite AnN_2 , and Rocksalt AnN ($An = U, Np$, and Pu). Table 2 reports the relative energy, lattice parameter, magnetic moment, and band gap for actinide nitrides (AnN_2 and AnN) using the HSE functional. If one takes nitrogen as trivalent, the stoichiometry of AnN_2 implies An^{6+} and $2N^{3-}$, suggesting a $5f^0$ configuration for U, $5f^1$ for Np, and $5f^2$ for Pu. This expectation is reflected in the absence of a magnetic moment for UN_2 (Table 2). It is a band insulator, with an HSE predicted gap of 1.5 eV (Figure 2), consistent with a zero magnetic moment. PBE and PBE+U also predict UN_2 to be an insulator with a band gap of 0.8 eV.

The HSE lattice constant of UN_2 underestimates the experimental value by ca. 0.09 Å. A strong mixing between the N 2p and U 5f levels is apparent in the HSE DOS, implying a more covalent interaction than in the analogous dioxide (see Figure 2).

On the other hand, the Np and Pu dinitrides are predicted to be ferromagnetic metals. The moments on the metal sites can be used to infer a Np valence intermediate between 5+ and 6+ (f^2 and f^1), and a Pu valence near 5+ (f^3), with some 4+ (f^4) character. Again, HSE and PBE+U predict NpN and PuN to be poor metals, while PBE provides more density at the Fermi level, indicative of good metals.

HSE predicts UN to be a metallic AFM, ordered along (100), in agreement with experiment.²² The calculated lattice constant (4.943 Å) is somewhat larger than the experimental data (4.890 Å), implying an underestimate of the delocalization (bandwidth), consistent with the observed overestimate of the magnetic moment by around 1.1 μ_B . Figure 3 shows the calculated density of states and band structure for UN, NpN , and PuN obtained with HSE, PBE, and PBE+U. Analyzing UN in more detail, the states near the Fermi level from HSE are mainly contributed from U 5f, and are well-separated from the N 2p/U 5f derived bands at higher binding energy. Interestingly, HSE significantly underestimates the DOS near the Fermi energy, in disagreement with photoemission, which sees a strong, narrow U 5f derived band at E_F .^{23,24} The predictions from PBE+U are qualitatively similar to HSE (see Figure 3). On the other hand, the DOS at E_F from the semilocal PBE approximation is in good agreement with

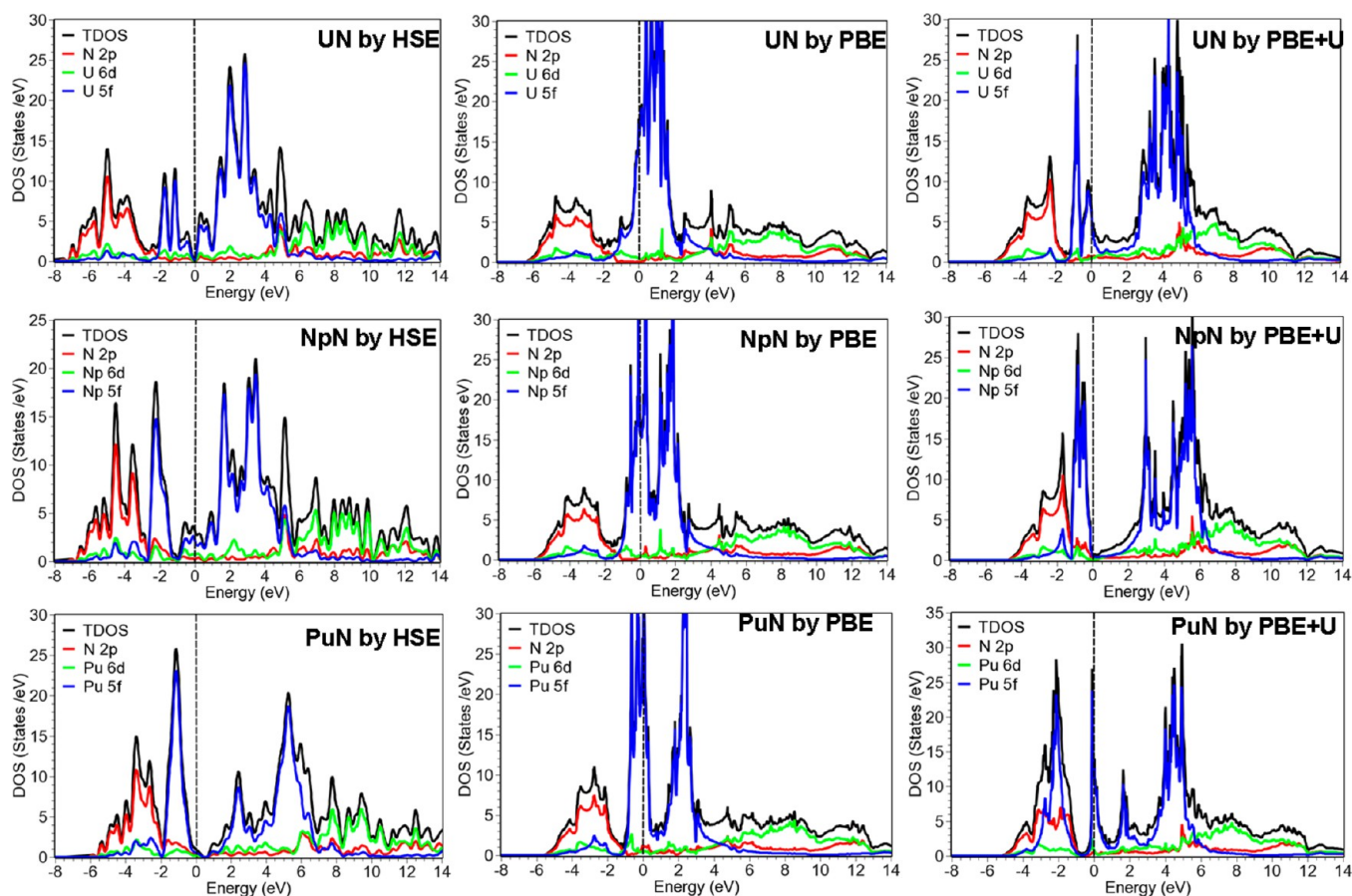


Figure 3. Calculated density of states of the corresponding most stable states of AnN ($\text{An} = \text{U}, \text{Np}$, and Pu) obtained with HSE, PBE, and PBE+U ($U_{\text{eff}} = 4 \text{ eV}$).

experiment. The lattice constant is also improved (see the Supporting Information). Unfortunately, PBE incorrectly yields a ferromagnetic ground state.

We surmise that the origin of the issues with the screened hybrid HSE and the PBE+U approximations is associated with the increased screening expected in a metallic system compared with an insulator. There is presently no means to “dynamically” screen either the effective Hubbard U in PBE+U, or the screening length in HSE “on the fly”. In HSE, the screening length ω is an adjustable parameter governing the extent of short-range interactions; the optimum value is approximately $0.2\text{--}0.3 \text{ \AA}^{-1}$. In current calculations, ω is set up to its standard value of 0.207 \AA^{-1} . As a numerical experiment, in order to test the sensitivity of our results on ω , we find that the density at the Fermi level increases with an increase of the screening parameter, suggesting that an approach in which the screening parameter is adjusted dynamically in response to the electronic structure would be very helpful for strongly correlated metals. Note that for $\omega = 0$, HSE reproduces PBE0 (up to a slight deviation due to the parametrization of the PBE exchange hole). HSE reduces to the nonhybrid PBE functional for $\omega \rightarrow \infty$. A value of $\omega = 1$ is effective in reproducing the experimental photoemission data (see the Supporting Information). We tentatively conclude that screened hybrid DFT is missing key physics in the correlated metal regime.

A number of other theoretical studies have addressed actinide mononitrides using approximations including GGA,^{25–27} LSDA,²⁸ LDA+U,²⁹ SIC,³⁰ and DMFT.³¹ The predicted lattice constants by these groups are all reasonably close to experiment

Table 2. Calculated Relative Energy (eV per AnN_2 or AnN , where $\text{An} = \text{U}, \text{Np}$, and Pu), Lattice Constants (\AA), Magnetic Moment (μ_B), and Band Gap (eV) Using HSE

		magn state	E_{rel} (eV per AnN_2)	a_0 (\AA)	μ (μ_B)	E_{gap} (eV)
AnN_2	UN ₂	AFM ^a	0.00	5.218	0.00	1.5
		FM	0.00	5.218		
		NM	0.00	5.218		
		expt		5.310 ¹⁶		
	NpN ₂	AFM ^a	0.00	5.187	1.59	0.0
		FM	−0.05	5.208	1.80	0.0
		NM	0.45	5.150		
		expt		—	—	—
	PuN ₂	AFM ^a	0.00	5.234	3.02	0.0
		FM	−0.53	5.244	3.25	0.0
		NM	1.10	5.148		
		expt		—		
AnN	UN	AFM ^a	0.00	4.943	1.82	0.0
		FM	0.22	4.860		
		NM	0.67	4.795		
		expt		4.890 ¹⁶	0.75 ¹⁹	
	NpN	AFM ^a	0.00	4.906	3.17	0.0
		FM	−0.05	4.936	3.51	0.0
		NM	2.09	4.769		
		expt		4.899 ²⁰		
	PuN	AFM ^a	0.00	4.978	4.80	0.0
		FM	0.04	5.013		
		NM	3.50	4.840		
		expt		4.905 ²¹		

^aA small tetragonal disorder with $a = b \neq c$ is found in AFM states.

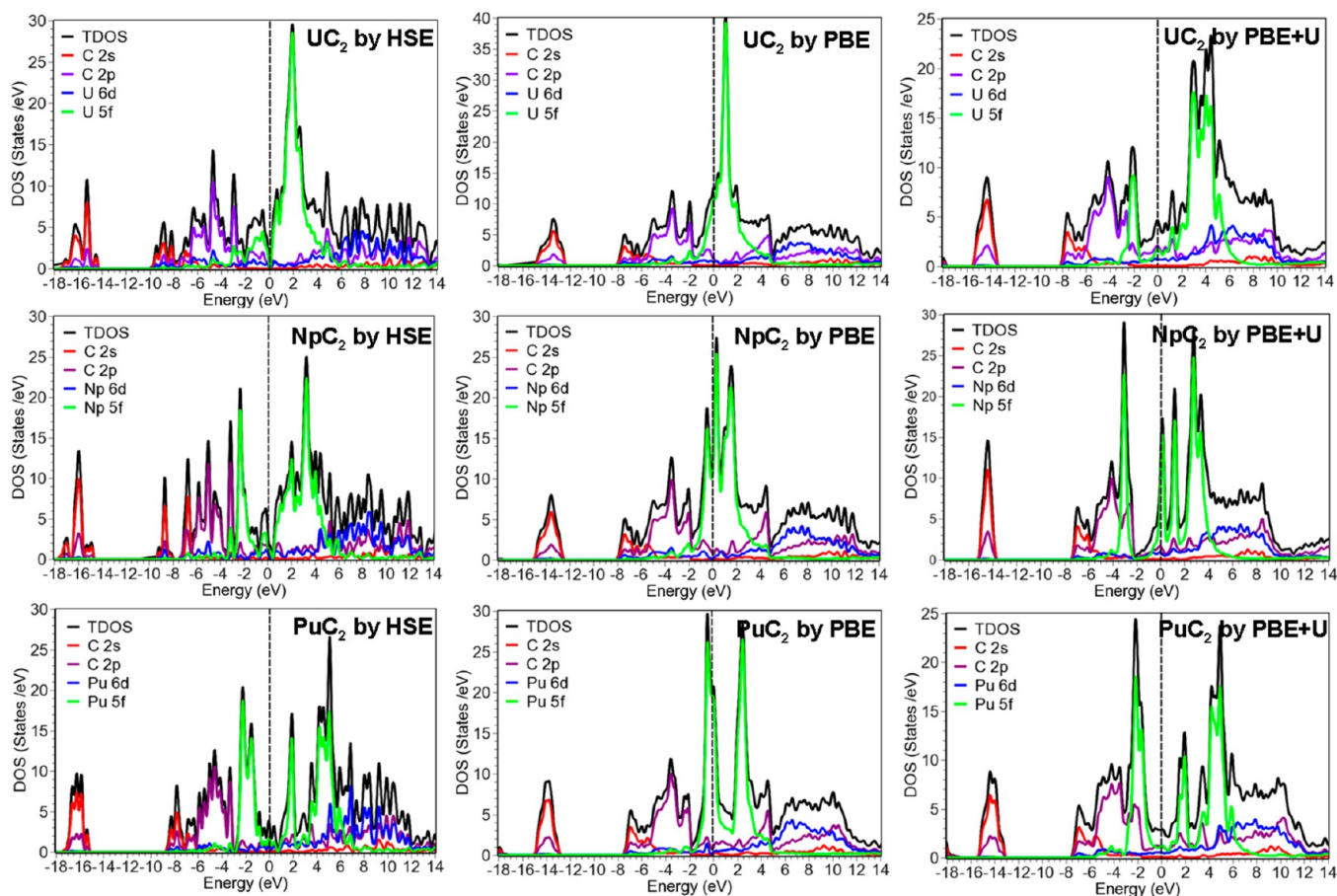


Figure 4. Calculated density of states of the corresponding most stable states of AnC_2 ($\text{An} = \text{U}, \text{Np}, \text{and Pu}$) obtained with HSE, PBE, and PBE+U ($U_{\text{eff}} = 4 \text{ eV}$).

Table 3. Calculated Relative Energy (eV per AnC_2 or AnC , where $\text{An} = \text{U}, \text{Np}, \text{and Pu}$), Lattice Constants (\AA), Magnetic Moment (μ_{B}), and Band Gap (eV) Using HSE

		magn state	$E_{\text{rel.}}$ (eV per AnC_2)	a_0/c_0 (\AA)	μ (μ_{B})	E_{gap} (eV)
AnC_2	UC_2	AFM	0.00	3.515/5.913	1.00	0.0
		FM	0.18	3.457/5.893	—	—
		NM	0.18	3.455/5.893	—	—
		expt	—	3.524/5.999 ¹⁶	—	—
NpC_2		AFM	0.00	3.626/6.085	3.16	0.0
		FM	0.02	3.635/6.078	—	—
		NM	0.02	3.635/6.078	—	—
		expt	—	—	—	—
PuC_2		AFM	0.00	3.758/6.263	4.99	0.0
		FM	0.07	3.769/6.273	—	—
		NM	3.33	3.499/5.916	—	—
		expt	—	—	—	—
		magn state	$E_{\text{rel.}}$ (eV per AnC)	a_0 (\AA)	μ (μ_{B})	E_{gap} (eV)
AnC	UC	AFM ^a	0.00	5.055	1.40	0.0
		FM	0.05	4.996	—	—
		NM	0.24	4.902	—	—
		expt	—	4.961 ¹⁶	—	—
NpC		AFM ^a	0.00	5.082	3.10	0.0
		FM	0.06	5.090	—	—
		NM	1.89	4.890	—	—
		expt	—	4.905 ²¹	—	—
PuC		AFM ^a	0.00	5.115	4.35	0.0
		FM	0.12	5.043	—	—
		NM	3.19	4.918	—	—
		expt	—	4.897 ¹⁷	—	—

^aA small tetragonal disorder with $a = b \neq c$ is found in AFM states.

(no lattice parameter from DMFT), as obtained in this work. Atta-Fynn and Ray²⁶ have shown that in full-potential GGA calculations there are no big differences on the structural and electronic properties with and without spin orbital coupling; their DOS is quite similar to those here reported with PBE. The electronic properties predicted for UN by SIC³⁰ and DMFT³¹ are quite similar to the results from PBE in the current work.

2.3. Actinide Carbides, CaC_2 Type AnC_2 , and Rocksalt AnC ($\text{An} = \text{U}, \text{Np}, \text{and Pu}$). Table 3 summarizes the calculated relative energies for AFM, FM, and NM states; lattice constants (\AA); magnetic moment (μ_{B}); and band gap (eV) of actinide carbides (CaC_2 type AnC_2 and rocksalt AnC) using HSE. A more detailed study on UC_2 phases has been published elsewhere.³² HSE predicts all actinide carbides to be metallic. It is interesting to note that HSE underestimates the lattice constant in the c direction for UC_2 , just as it did for UN_2 . This is in contrast with the overestimates observed for the monoxides and mononitrides. In fact, it returns to form in the monocarbides, once again overestimating the bond lengths, presumably implying an overestimate of electron localization. The DOS at E_{f} is once again predicted to be rather small with HSE (see Figures 4 and 5), but greater in PBE, in agreement with the DMFT results.³¹

3. CONCLUSIONS

The structural, electronic, and magnetic properties of actinide oxides, nitrides, and carbides (AnX_{1-2} with $\text{X} = \text{C}, \text{N}, \text{O}$) have

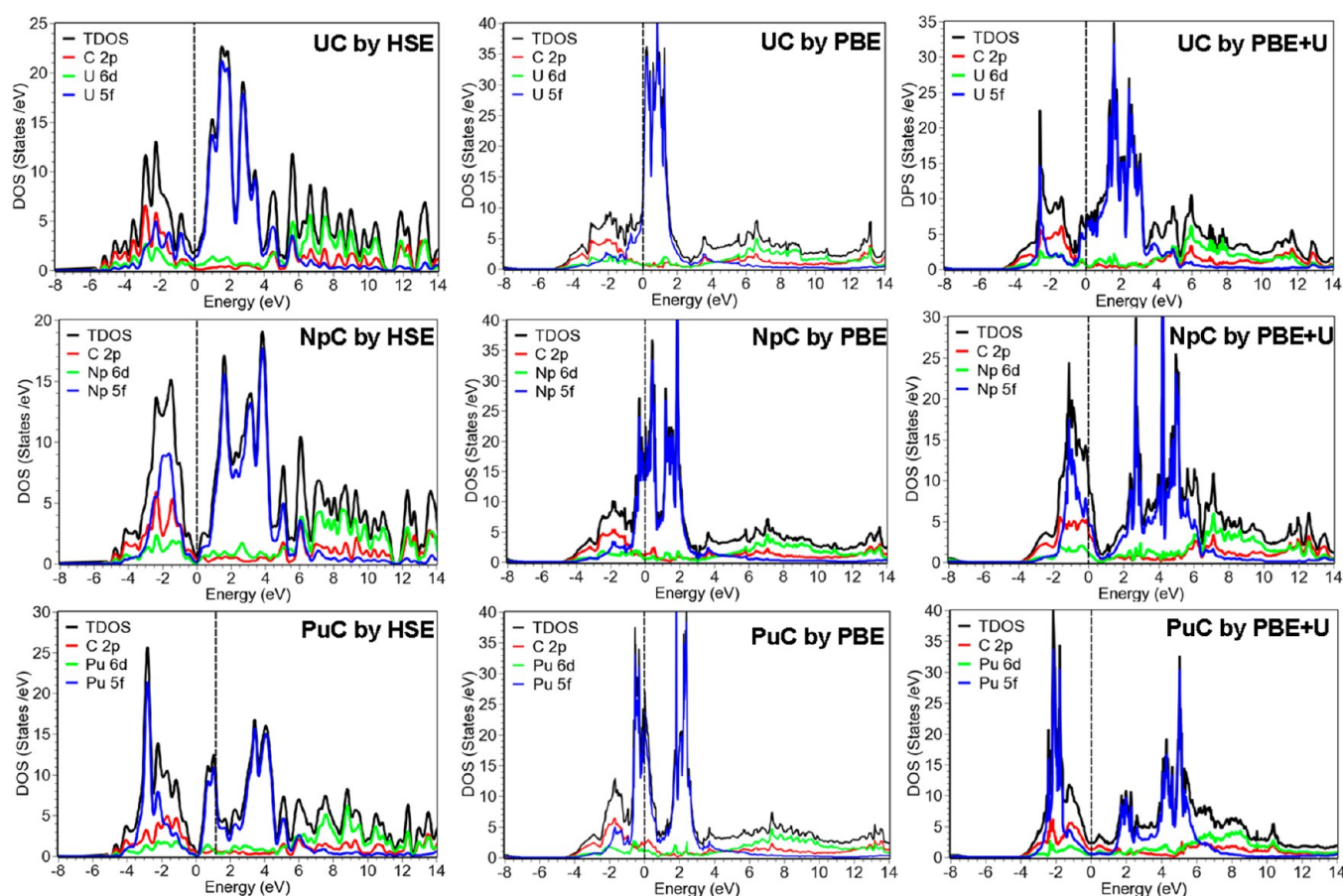


Figure 5. Calculated density of states of the corresponding most stable states of AnC (An = U, Np, and Pu) obtained with HSE, PBE, and PBE+U ($U_{\text{eff}} = 4$ eV).

been systematically investigated using the HSE, PBE, and PBE+U approximations. While the screened hybrid HSE functional seems clearly superior for the strongly correlated actinide dioxide insulators, its performance for the metallic nitrides and carbides is problematic, at least with respect to the densities-of-states. For properties other than magnetism, the semi-local PBE approximation gives an improved description of the properties, particularly the photoemission data. We conclude that a satisfactory approximation which smoothly interpolates from the limit of a simple metal to a strongly correlated Mott insulator remains a challenge in electronic structure theory.

■ ASSOCIATED CONTENT

Supporting Information

Section I, electronic properties of actinide oxides, nitrides, and carbides, a screened hybrid DFT study (HSE); section II, electronic properties of actinide oxides, nitrides and carbides, a PBE study; section III, electronic properties of actinide oxides, nitrides, and carbides, a PBE+U study; section IV, effect of screening length (ω) on the electronic and structural properties of UN. This material is available free of charge via the Internet at <http://pubs.acs.org>

■ AUTHOR INFORMATION

Corresponding Author

*Phone: 505-667-7096. E-mail: rlmartin@lanl.gov.

Notes

The authors declare no competing financial interest.

■ ACKNOWLEDGMENTS

This work was supported under the Heavy Element Chemistry Program at Los Alamos National Laboratory by the Division of Chemical Sciences, Geosciences, and Biosciences, Office of Basic Energy Sciences, U.S. Department of Energy. Portions of the work were also supported by the LDRD program at Los Alamos National Laboratory. X.-D.W. gratefully acknowledges a Seaborg Institute Fellowship. The work at Rice University is supported by DOE, Office of Basic Energy Sciences, Heavy Element Chemistry program, under Grant DEFG02-04ER15523. Some of the calculations were performed on the Chinook computing systems at the Molecular Science Computing Facility in the William R. Wiley Environmental Molecular Sciences Laboratory (EMSL) at PNNL. Some of the calculations were done on LOBO supercomputer of High Performance Computing at Los Alamos National Laboratory. The Los Alamos National Laboratory is operated by Los Alamos National Security, LLC, for the National Nuclear Security Administration of the U.S. Department of Energy under Contract DE-AC5206NA25396.

■ REFERENCES

- (1) Butler, D. Energy: Nuclear Power's New Dawn. *Nature* **2004**, 429, 238–240.
- (2) Wen, X.-D.; Martin, R. L.; Roy, L. E.; Scuseria, G. E.; Rudin, S.; Batista, E. R.; McCleskey, T. M.; Joyce, J. J.; Scott, B. L.; Bauer, E.; Durakiewicz, T. Effect Of Spin-Orbit Coupling on the Actinide

Dioxides AnO_2 ($\text{An} = \text{Th}, \text{Pa}, \text{U}, \text{Np}, \text{Pu}, \text{and Am}$): A Screened Hybrid Density Functional Study. *J. Chem. Phys.* **2012**, *137*, 154707.

(3) Wen, X.-D.; Martin, R. L.; Henderson, T. M.; Scuseria, G. E. Density Functional Theory Studies of the Electronic Structure of Solid State Actinide Oxides. *Chem. Rev.* **2013**, *113*, 1063–1096.

(4) Wen, X.-D.; Martin, R. L.; Scuseria, G. E.; Rudin, S. P.; Batista, E. R.; Burrell, A. K. Screened Hybrid and DFT + U Studies of the Structural, Electronic, and Optical Properties of U_3O_8 . *J. Phys. Cond. Matter.* **2013**, *25*, 025501.

(5) Heyd, J.; Scuseria, G. E.; Ernzerhof, M. Hybrid Functionals Based on a Screened Coulomb Potential. *J. Chem. Phys.* **2003**, *118*, 8207.

(6) Kresse, G.; Hafner, J. Ab Initio Molecular Dynamics for Liquid Metals. *Phys. Rev. B* **1993**, *47*, 558.

(7) Heyd, J.; Scuseria, G. E.; Ernzerhof, M. Erratum: “Hybrid Functionals Based on a Screened Coulomb Potential” [*J. Chem. Phys.* **118**, 8207 (2003)]. *J. Chem. Phys.* **2006**, *124*, 219906.

(8) Schoenes, J. Optical Properties and Electronic Structure of UO_2 . *J. Appl. Phys.* **1978**, *49*, 1463.

(9) Los Alamos Science; Cooper, N. G., Ed.; Los Alamos National Laboratory: Los Alamos, NM, 2000; Vol. 26.

(10) Kern, S.; Robinson, R. A.; Nakotte, H.; Lander, G. H.; Cort, B.; Wason, P.; Vigil, F. A. Crystal-Field Transition in PuO_2 . *Phys. Rev. B* **1999**, *59*, 104.

(11) Yamashita, T.; Nitani, N.; Tsuji, T.; Inagaki, H. Thermal Expansion of Neptunium–Uranium Mixed Oxides. *J. Nucl. Mater.* **1997**, *247*, 90–93.

(12) Eedös, P.; Solt, G.; Zolnieriek, A.; Blaise, A.; Fournier, J. M. Magnetic Susceptibility and the Phase Transition of NpO_2 . *Phys. B+C* **1980**, *102*, 164–170.

(13) McCleskey, T. M.; Bauer, E.; Jia, Q.; Burrell, A. K.; Scott, B. L.; Conradson, S. D.; Mueller, A.; Roy, L. E.; Wen, X.-D.; Scuseria, G. E.; Martin, R. L. Optical Band Gap of NpO_2 and PuO_2 from Optical Absorbance of Epitaxial Films. *J. Appl. Phys.* **2013**, *113*, 013515.

(14) Haschke, J. M.; Allen, T. H.; Morales, L. A. Reaction of Plutonium Dioxide with Water: Formation and Properties of PuO_{2+x} . *Science* **2000**, *287*, 285–287.

(15) Yasuoka, H.; Koutroulakis, G.; Chudo, H.; Richmond, S.; Veirs, D. K.; Smith, A. I.; Bauer, E. D.; Thompson, J. D.; Jarvinen, G. D.; Clark, D. L. Observation of ^{239}Pu Nuclear Magnetic Resonance. *Science* **2012**, *336*, 901–904.

(16) Rundle, R. E.; Baenziger, N. C.; Wilson, A. S.; McDonald, R. A. The Structures of the Carbides, Nitrides and Oxides of Uranium. *J. Am. Chem. Soc.* **1948**, *70*, 99–105.

(17) Zachariasen, W. H. Crystal Chemical Studies of the *Sf*-Series of Elements. XII. New Compounds Representing Known Structure Types. *Acta Crystallogr.* **1949**, *2*, 388–390.

(18) Chikalla, T. D.; McNeilly, C. E.; Skavdahl, R. E. The Plutonium–Oxygen System. *J. Nucl. Mater.* **1964**, *12*, 131–141.

(19) Erdos, P.; Robinson, J. M. *Actinide Compounds*; Plenum Press: New York, 1983.

(20) Olson, W. M.; Mulford, R. N. R. The Melting Point and Decomposition Pressure of Neptunium Mononitride. *J. Phys. Chem.* **1966**, *70*, 2932–2934.

(21) Tennery, V. J.; Bomar, E. S. Lattice Parameters of (U, Pu)N Solid Solutions. *J. Am. Ceram. Soc.* **1971**, *54*, 247–249.

(22) Curry, N. A. An Investigation of Magnetic Structure of Uranium Nitride by Neutron Diffraction. *Proc. Phys. Soc. London* **1965**, *86*, 1193–1198.

(23) Norton, P. R.; Tapping, R. L.; Creber, D. K.; Buyers, W. J. L. Nature of the *Sf* Electrons in Uranium Nitride: A Photoelectron Spectroscopic Study of UN, U, UO_2 , ThN, and Th. *Phys. Rev. B* **1980**, *21*, 2572.

(24) Samsel-Czekala, M.; Talik, E.; Du Plessis, P. de V.; Troé, R.; Misioriek, H.; Sulkowski, C. Electronic Structure and Magnetic and Transport Properties of Single-Crystalline UN. *Phys. Rev. B* **2007**, *76*, 144426.

(25) Sedmidubsky, D.; Konings, R. J. M.; Novak, P. Calculation of Enthalpies of Formation of Actinide Nitrides. *J. Nucl. Mater.* **2005**, *344*, 40–40.

(26) Atta-Fynn, R.; Ray, A. K. Density Functional Study of the Actinide Nitrides. *Phys. Rev. B* **2007**, *76*, 115101.

(27) Shibata, H.; Tsuru, T.; Hirata, M.; Kaji, Y. First Principles Study on Elastic Properties and Phase Transition of NpN . *J. Nucl. Mater.* **2010**, *401*, 113–117.

(28) Brooks, M. S. S.; Kelly, P. Large Orbital-Moment Contribution to *Sf* Band Magnetism. *J. Phys. Rev. Lett.* **1983**, *51*, 1708–1711.

(29) Ghosh, D. B.; De, S. K.; Oppeneer, P. M.; Brooks, M. S. S. Electronic Structure and Optical Properties of Am Monopnictides. *Phys. Rev. B* **2005**, *72*, 115123.

(30) Petit, L.; Svane, A.; Szotek, Z.; Temmerman, W. M.; Stocks, G. M. Ground-State Electronic Structure of Actinide Monocarbides and Mononitrides. *Phys. Rev. B* **2009**, *80*, 045124.

(31) Yin, Q.; Kutepov, A.; Haule, K.; Kotliar, G.; Savrasov, S. Y.; Pickett, W. E. Electronic Correlation and Transport Properties of Nuclear Fuel Materials. *Phys. Rev. B* **2011**, *84*, 195111.

(32) Wen, X.-D.; Rudin, S. P.; Batista, E. R.; Clark, D. L.; Scuseria, G. E.; Martin, R. L. Rotational Rehybridization and the High Temperature Phase of UC_2 . *Inorg. Chem.* **2012**, *51*, 12650–12659.